crystals

MDPI

Article

Determination of the Relationship between Proportional and Non-Proportional Fatigue Damage in Magnesium Alloy AZ31 BF

Vitor Anes [1,2,3,*], Francisco Bumba [3], Luís Reis [3] and Manuel Freitas [3]

[1] Instituto Superior de Engenharia de Lisboa, 1959-007 Lisboa, Portugal
[2] Instituto Politécnico de Lisboa, 1549-020 Lisboa, Portugal
[3] IDMEC, Instituto Superior Técnico, Universidade de Lisboa, 1049-001 Lisboa, Portugal
* Correspondence: vitor.anes@isel.pt

Abstract: In this work, the magnesium alloy AZ31BF subjected to proportional and non-proportional loads has been studied. For this purpose, a series of experimental multiaxial fatigue tests were carried out according to the ASTM E466 protocol. The main objective was to determine the relationship between the multiaxial fatigue strength of this alloy under these two different types of loading. The results showed that the AZ31BF magnesium alloy has different fatigue strengths depending on the loading type. Based on these results, it was found that the ratio between proportional and non-proportional damage in AZ31BF magnesium alloy varies depending on the number of loading cycles. To represent this variation, parameter Y was used to modulate the non-proportional damage of AZ31BF. In this way, two Y functions were considered, one for the normal stress component and the other for the shear stress component. The results obtained for the non-proportional parameter Y are of particular interest since the multiaxial fatigue models do not distinguish between these two types of loading when evaluating fatigue life. In this sense, the results of this study can be used in these models to overcome this limitation.

Keywords: magnesium alloys; multiaxial fatigue; non-proportional loading; experimental testing

Citation: Anes, V.; Bumba, F.; Reis, L.; Freitas, M. Determination of the Relationship between Proportional and Non-Proportional Fatigue Damage in Magnesium Alloy AZ31 BF. *Crystals* **2023**, *13*, 688. https://doi.org/10.3390/cryst13040688

Academic Editor: Bolv Xiao

Received: 27 March 2023
Revised: 12 April 2023
Accepted: 14 April 2023
Published: 17 April 2023

1. Introduction

The transportation industry is a major contributor to CO_2 emissions, leading to increased global warming and lower quality of life in societies as pollution increases, which in turn negatively impacts public health. This fact is closely related to the weight of vehicles. The higher the weight, the higher the fuel consumption, and the higher the emission of CO_2 [1].

In this sense, over the years, the transportation industry, especially the automotive and aeronautical industries, have explored the use of lighter materials in their vehicles in order to reduce their weight, thus reducing fuel consumption and, consequently, CO_2 emissions [2]. This strategy is in line with the 17 Sustainable Development Goals of the United Nations, as it not only promotes the sustainability of the planet but also that of secondary industries, especially those that use vehicles as a fundamental means of doing business.

However, despite these efforts, the strategies are still far from fully achieving the goals. For example, in recent decades, the aerospace industry has invested heavily in building aircraft from composite materials, particularly carbon fiber, because of their high mechanical strength and low weight. However, due to the uncertainty about the mechanical properties of these materials, the safety coefficients are very high, which leads to an oversizing of the structures, which, in turn, leads to an increase in weight. In this way, results in aircraft weight reduction have fallen far short of expectations [3,4].

On the other hand, the cost of manufacturing and maintaining these structures is much higher than for aluminum alloy structures, resulting in a more expensive solution. This fact has encouraged the continued use of aluminum alloys in aircraft construction, as there is a high demand due to economic factors [5].

In this context, magnesium alloys are proving to be an alternative to both carbon fiber composites, steel, and aluminum alloys. Magnesium alloys are about 75% lighter than steel, 50% lighter than titanium, and 33% lighter than aluminum. Compared to carbon fiber composites, magnesium alloys are about 20% heavier, but the energy costs associated with that 20% are fully recovered at the end of the product's life [6,7].

Looking at the life cycle of the products, magnesium alloys are fully recyclable, while composites are not. So, the decommissioning and disposal of scrap at the end of the life cycle of carbon fiber structures incurs higher costs and contributes to CO_2 emissions, which to some extent, negates the advantage that they are 20% lighter than magnesium alloys. However, magnesium alloy structures are cheaper to manufacture and maintain, which, in turn, makes the purchase and maintenance costs more attractive to the end user [8].

In addition to structural applications, magnesium alloys can also be used in dentistry, for example, for temporary implants [9]. Magnesium alloys are non-toxic to the human body and biodegradable, i.e., the human body gradually degrades the mass of the implant until it is completely eliminated from the body.

Due to this property, i.e., the natural and gradual degradation of the implant over time, the challenge is to size the implant to ensure its structural resistance during the time it takes the body to recover.

The sizing of dental implants is a major challenge in itself [10–12]. However, this challenge becomes significantly greater when these implants are made of magnesium alloys, as the variations in mechanical strength, resulting from the structural reduction of the implant due to removal by the body, must be taken into account.

Despite the above advantages, magnesium alloys present some challenges in characterizing their mechanical behavior. Over time, some challenges have been solved, such as the problem of corrosion. The new magnesium alloys have corrosion resistance comparable to that of aluminum alloys, so corrosion is no longer a major problem in magnesium alloys. However, due to the peculiarities of their crystalline structure, magnesium alloys have a different mechanical behavior than aluminum and steel alloys. For this reason, the design of magnesium alloy mechanical components or structures requires additional information beyond that required for other structural materials [13].

A unique property of magnesium alloys is that they exhibit differential compressive and tensile yield stresses, a property not found in other structural materials. This property results from their hexagonal close-packed crystalline structure (HCP), which allows them to accommodate very specific slip planes at the microstructural level in a form known as twinning, in which the microstructure has a mirrored morphology in a specific direction, which has implications for the mechanical response to cyclic loading [14,15].

Another characteristic feature is the hysteresis cycles that occur during cyclic loading. It can be seen that the hysteresis loops are not symmetrical with respect to the reference axes, as is the case with other structural materials. This asymmetry results from the different behavior of magnesium alloys in tension and compression. In tension, magnesium alloys tend to harden cyclically, i.e., the cyclic yield stress tends to increase with the number of loads, while in compression the variation of the cyclic yield stress is almost zero [16].

These aspects of the mechanical behavior of magnesium alloys have been systematically studied over time. However, there are some gaps in the literature regarding the resistance of magnesium alloys to multiaxial cyclic loading, i.e., the information available in the literature on the multiaxial fatigue strength of magnesium alloys is somewhat limited. In this sense, further studies are needed to fill this important gap, especially with respect to the influence of the loading paths' nature on fatigue strength [17].

In practice, structures are usually subjected to random loading spectra of multiaxial nature, which are characterized by fatigue damage accumulation models during the development of structures and mechanical components. Therefore, the characterization of the mechanical behavior of magnesium alloys in multiaxial loading regimes is extremely important to ensure the required reliability of magnesium structures [18].

In practice, load spectra can be determined in the field by instrumenting the structure or by using databases of previously recorded load spectra, such as the FALSATFF database. These load spectra summarize cyclic loads of different types that cause various degrees of damage. The load spectra can summarize uniaxial cyclic loads (normal and shear and with or without mean stress) and multiaxial loads (proportional and non-proportional, with or without mean stress, and synchronous or asynchronous) [19].

The results presented in the literature for different structural materials show that the multiaxial fatigue strength strongly depends on the type of loading, i.e., for the same stress level (e.g., for the same von Mises equivalent stress), the fatigue strength of a given material is different depending on the loading path. In addition to this proof, the loading sequence (sequential combination of different types of loading) also has a strong influence on the fatigue strength of materials [20].

Another important aspect is the limitation of damage parameters when distinguishing the loading type. For example, multiaxial fatigue models based on the invariant of the stress tensor consider only the amplitude ranges of the normal and shear stresses. This results in the same damage value for proportional and non-proportional loads if they have the same amplitude ranges. However, it has been experimentally demonstrated that the damage caused by these loads is different, resulting in different fatigue lives [21].

With this in mind, and for a given material, it is extremely important to characterize these loads in terms of their resistance to multiaxial fatigue, both individually and in aggregate form, to facilitate decision-making in the design of the structures subjected to load spectra. This characterization is of particular importance in magnesium alloys because the information available in the literature on the effects of loading type on resistance to multiaxial fatigue is almost non-existent. In particular, the fatigue resistance of magnesium alloys subjected to non-proportional loads is very limited.

The objective of this article is to characterize the relationship between damage due to proportional loading and damage due to non-proportional loading in AZ31BF magnesium alloy. To our knowledge, this relationship has never been studied in magnesium alloys, although it is of great importance for the evaluation of cumulative damage in multiaxial loading spectra.

To obtain this relationship, a series of experimental tests were performed considering two reference loads, namely a proportional load with an amplitude ratio of 45º and a non-proportional load with an amplitude ratio of 45º and a phase shift angle between normal and shear stress of 90 degrees. For these two loads, the ratio between the amplitudes of the normal and shear stresses is the same. The only difference between the loads is the phase shift angle between normal and shear stresses, which is present in the non-proportional load.

The paper is divided into five sections, starting with an introduction that introduces the reader to the research problem with a holistic approach, covering topics ranging from the impact on the industry to the research question that this paper aims to answer. Then, the Literature Review section presents the most commonly used theoretical approaches to characterize non-proportional loads. In the Materials and Methods section, the methodology used in the experimental tests and a brief characterization of the material in question are presented. The Results section presents the findings, the Discussion section discusses the results obtained, and the Conclusions section concludes the paper.

2. Literature Review

The loading path results from the combination of normal and shear stresses that can load the material in many different ways. Materials respond differently depending on the loading path even at the same stress level. This is because multiaxial fatigue strength is strongly related to the shape of the loading path [22].

Essentially, there are two types of loading by which all cyclic loading can be characterized: proportional and non-proportional. The main feature that distinguishes the two types of loading is the variation in the principal directions of the stress tensor. In non-proportional loads, the main directions of the stress tensor change during the duration of the load, while in proportional loads they remain constant or unchanged. As for the effect of the load on the material, these two types of loads cause different fatigue damage. In proportional loads, the material is loaded in a certain plane (direction) given by the ratio of the stress amplitudes. Non-proportional loads, on the other hand, activate more than one stress plane in the material, resulting in non-proportional loads causing additional phenomenological effects, such as non-proportional hardening [23].

Material hardening is the phenomenological response of the material to external stresses, and it is particularly sensitive to the intensity of stress and the type of stress. Essentially, internal microplasticity due to cyclic loading alters material strength, fatigue behavior, and cracking. Therefore, during the initial loading cycles, materials seek a stable response, i.e., a stress–strain relationship that corresponds to the type of external loading [24].

After the material has cyclically adapted to the initial loading cycles, the stress state is maintained for the remainder of the loading period if the loading pattern is not changed in the interim. Under strain control conditions, material hardening results in an increase in the stress level required to maintain the same strain amplitude, i.e., the cyclic strain is maintained during the loading period when the loading level is increased [25].

On the other hand, a constant stress amplitude during stress-controlled loading results in a decrease in strain amplitude due to material hardening. This point is very important because material accommodation (or response to loading) affects the stress state. Therefore, the relationship between stresses and strains becomes nonlinear during elastic cyclic loading.

On the other hand, softening of the material by cyclic loading is the opposite phenomenon described in the concept of cyclic hardening. In this case, and from the point of view of stress control, constant stress amplitudes increase the inherent strain amplitude in materials that soften cyclically, which can lead to higher plasticity. In addition, higher strains increase the potential for cracking. Therefore, this type of material is much more susceptible to failure than materials that harden cyclically. Nevertheless, construction materials do usually harden. Therefore, this issue, cyclic softening, is not as much of a focus in the literature as the phenomenon of cyclic curing.

Analyzing the state of assessing non-proportional cyclic damage, one can conclude that the general way to deal with non-proportionality is to find a factor that corrects the damage parameter criterion in some way [25,26].

None of the multiaxial fatigue criteria found in the literature account for non-proportional cyclic effects by default. Multiaxial fatigue criteria are generally insensitive to non-proportionality, i.e., the criteria procedures do not distinguish between proportional and non-proportional loading conditions. For this reason, without any correction, their fatigue life estimates show an unsatisfactory correlation with test data.

There are several physical phenomena in non-proportional loading that add complexity to the fatigue damage assessment for this type of loading. These phenomena result from different types of non-proportionality that can arise from a loading path, such as non-proportionality due to loading sequences, variable amplitude, and mean stresses [27].

Therefore, finding a damage parameter that captures the additional damage due to non-proportionality remains a difficult task. Non-proportionality is closely related to the nature of the loading path and, therefore, has been evaluated in the literature based on the shape of the loading path.

The non-proportionality of materials is usually characterized on the basis of the non-proportional cyclic hardening coefficient of the material [28,29].

This coefficient is usually determined considering two specific multiaxial loading cases, namely: the non-proportional loading with a phase shift of 90 degrees and a stress amplitude ratio of 45 degrees, and the typical proportional loading with a stress amplitude ratio of 45 degrees and a phase shift of zero (the stress amplitude ratio is evaluated in the von Mises stress space).

For each (proportional and non-proportional) equivalent total strain within a predefined strain range, the equivalent stress values under proportional and non-proportional loading conditions are investigated. These values are determined when cyclically stable behavior is achieved at each total strain and used to measure the non-proportional response (behavior) of the material to non-proportional loading.

To evaluate the non-proportionality, some coefficients have been proposed in the literature. The non-proportional hardening coefficient α is one example [30].

This coefficient tries to capture the maximum non-proportional effect by considering the ratio between the non-proportional equivalent stress (90 degrees out of phase and with a stress amplitude ratio of 45 degrees) and the proportional equivalent stress (with a stress amplitude ratio of 45 degrees). In order to determine the values of the two equivalent stresses and evaluate the non-proportional strain hardening coefficient alfa, stabilized stress–strain curves must be obtained by experiments before evaluating the equivalent stresses. The expression for the non-proportional strain hardening α is as follows in Equation (1).

$$\alpha = \frac{\sigma_{eqv,OP}}{\sigma_{eqv,PP}} - 1, \tag{1}$$

where *PP* stands for proportional and *OP* for non-proportional. In order to generalize the α parameter for any kind of non-proportional loading cases, Socie and Marquis [30] developed the idea that the entire loading path represented in a stress space can be enclosed by an ellipse. Then, the ratio between the minor (b) and major (a) axes of the ellipse enclosing the stress path is the so-called non-proportional factor F, given by the following Equation (2):

$$F = \frac{b}{a}. \tag{2}$$

This factor has been used to quantify the degree of non-proportionality within a stress path, which is used to correlate the non-proportional cyclic hardening behavior of the material. These two coefficients, α and F, can be used to update equivalent stress to account for the phenomenological behavior of a given material under non-proportional loads. Equation (3) shows this update.

$$\overline{\sigma} = K' \cdot (1 + \alpha \cdot F) \cdot \left(\overline{\varepsilon_p}\right)^{n'}, \tag{3}$$

where α is the non-proportional strain hardening coefficient, ε_p is the plastic strain, F is the non-proportionality factor, and K' and n' are the coefficient and exponent of the stress–strain curve equation, respectively.

Based on experiments, Anes et al. [31] found that the axial and shear S-N curves are nearly parallel to each other under proportional and non-proportional loading when the ratio of stress amplitudes is equal to $1/\sqrt{3}$. This result suggests that the relative position between the axial and shear S-N curves under proportional and non-proportional loading is due to the non-proportional contribution to the total fatigue damage.

Furthermore, the relative damage between proportional and non-proportional loading can be considered constant and independent of fatigue life, since both the proportional and non-proportional S-N curves are parallel to each other. The physical significance of the relative damage between proportional and non-proportional load curves is justified as follows:

If the S-N curves of the axial and shear components of a non-proportional load are above their homologous proportional curves, then for a given fatigue life it is necessary to increase the stress amplitude level of the non-proportional axial and shear components to obtain the same fatigue life. Therefore, in this scenario, the non-proportional load has a longer fatigue life than the proportional load, with the same axial and shear stress amplitudes for the proportional and non-proportional loads. In this scenario, the non-proportional load is less damaging than the proportional load, indicating that the material is less sensitive to non-proportionality.

On the other hand, if the axial and shear S-N curves of a non-proportional load are below their homologous proportional curves, the energy that must be expended for the fatigue damage process is less for non-proportional loading than for proportional loading. In this case, the non-proportional load is more damaging than the proportional load, indicating that the material is more sensitive to non-proportionality. To quantify the non-proportional sensitivity of the material, Anes et al. proposed the Y parameter, which correlates proportional and non-proportional loading amplitudes, and the non-proportional S-N curves (axial and shear) can be estimated with this parameter based on the proportional curves. Equations (4) and (5) show the Y parameter in relation to the S-N amplitudes for normal and shear stresses.

$$Y_{normal} = \frac{\sigma_{PP}}{\sigma_{OP}}, \tag{4}$$

$$Y_{shear} = \frac{\tau_{PP}}{\tau_{OP}}. \tag{5}$$

σ_{PP}, σ_{OP} stands for the amplitude of the normal stress and τ_{PP}, τ_{OP} for the amplitude of the shear stress. The difference between the alpha parameter and the Y parameter is based on the fact that the α parameter requires equivalent stress to evaluate non-proportional damage, using compatibility constants for the amplitudes of the normal and shear stresses. This fact may bias the interpretation of non-proportional damage to some extent. The Y parameter, on the other hand, does not use any equivalent stress. In this case, the non-proportional damage is evaluated by a strict comparison of the proportional and non-proportional amplitudes for the same fatigue duration.

The interpretation of the Y parameter is as follows: Thus if the Y-parameter has a value of less than 1, the material is less sensitive to non-proportionality than to proportionality. If the Y parameter is equal to 1, then proportional and non-proportional loads have the same effect on the fatigue strength of the material. When the Y parameter is greater than 1, the material can be considered to be very sensitive to the non-proportional loading conditions. In this case, the non-proportional loads have lower stress amplitudes than the proportional loads for a given fatigue life.

In this article, we intend to evaluate experimentally the parameter Y for the magnesium alloy AZ31BF. This parameter will allow for the estimation of the non-proportional damage based on the loading history and to understand the sensitivity of this alloy to non-proportional loading. This alloy has been studied extensively in recent years due to its potential for structural applications. These studies have focused on the cyclic response at low and high fatigue cycles, under uniaxial and multiaxial loading conditions [32–35], damping properties [36], elastic–plastic evolution at multiaxial loading conditions [13,14], modulation of cyclic response [37], and other topics. However, the relationship between proportional and non-proportional damage in AZ31BF magnesium alloy is not available in the literature, although it is extremely important for the evaluation of damage accumulation in variable amplitude spectra. In this sense, this work aims to fill this gap.

3. Materials and Methods

The experimental program began with the fabrication of the test specimens, followed by the selection of the load paths, and finally, the experimental tests were performed using the 8874 biaxial fatigue testing machines (Instron, Norwood, MA, USA). The test specimens consisted of bars made of AZ31BF magnesium alloy with a length of 1 m and a diameter of 26 mm. These bars were previously produced by extrusion of ingots at a temperature in the range of 360 to 380 °C and a speed of 51 mm/s, the final extrusion ratio being 6. After extrusion, the bars were hardened in air. Figure 1 shows the geometry of the specimens and their respective dimensions. The test specimens were manufactured on a CNC machine in compliance with the dimensions specified in the ASTM E 466 standard.

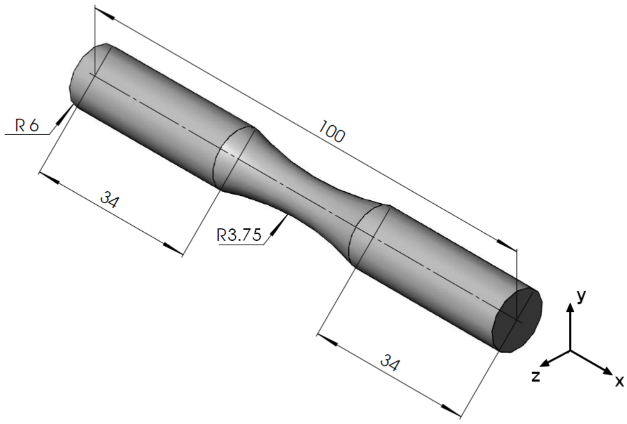

Figure 1. Specimen geometry and respective dimensions in (mm) [38].

During machining, the longitudinal direction of the test specimens was aligned with the longitudinal direction of the bars, i.e., with the extrusion direction of the bars. Surface finishing was first performed with abrasive paper of decreasing grit size and later with diamond paste to obtain a mirror-smooth surface. The fatigue tests were carried out under tensile load according to the procedures of ASTM E466, considering the two reference load paths normally used to evaluate resistance to multiaxial fatigue, namely proportional loading with *SAR* = 45, represented as *PP* (Figure 2a), and non-proportional loading with *SAR* = 45° and a displacement of 90°, represented as *OP*, (Figure 2b).

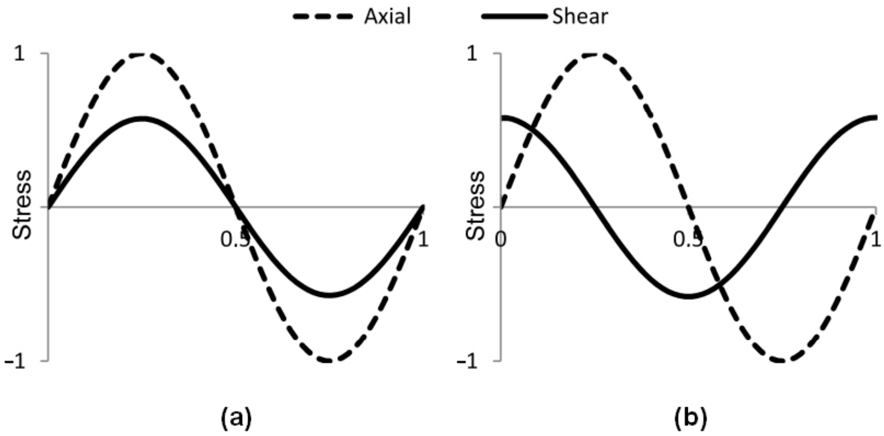

Figure 2. (**a**) Proportional loading time variation, and (**b**) non-Proportional loading time variation.

These loads have two load channels, one for torque and one for axial force. In each of the channels, a sine wave with R = −1 has been considered, i.e., the average stress is zero in both the normal stress channel and the shear stress channel. The condition for the end of the test and the recording of the respective fatigue life was the complete separation of the test specimen.

4. Results

The results of the experimental tests are shown in Tables 1 and 2 for proportional (*PP*) and non-proportional loading (*OP*), respectively. In both cases, care was taken to ensure that the ratio between the amplitudes of the shear and normal stresses was equal to 0.58. This ensured that the non-proportional damage, as assessed by the results shown in Table 2, resulted only from the phase shift between the amplitudes of the normal and shear stresses, thus avoiding other factors that could potentially distort the intended results.

Table 1. Fatigue life results for AZ31BF at proportional reference load (*PP*).

σ_a [MPa]	τ_a [MPa]	Phase Shift	SAR	*Nf*
106.07	61.24	0	0.58	16,800
91.92	53.07	0	0.58	46,878
77.78	44.91	0	0.58	69,169
74.25	42.87	0	0.58	242,685
70.71	40.82	0	0.58	353,718
67.18	38.78	0	0.58	1,000,000

Table 2. Fatigue life results for AZ31BF at non-proportional reference load (*OP*).

σ_a [MPa]	τ_a [MPa]	Phase Shift	SAR	*Nf*
106.07	61.24	90	0.58	7182
95.00	54.85	90	0.58	8595
74.25	42.87	90	0.58	167,525
72.50	41.86	90	0.58	576,336
70.71	40.82	90	0.58	800,000
67.18	38.78	90	0.58	1,000,000

The tables show, in the first column, the intensity of the amplitude of normal stress, in the second column, the intensity of the amplitude of shear stress, and in the third column, the phase shift of the load (proportional loads have a phase shift equal to zero), the next column shows the ratio between the intensity of the shear amplitude and the intensity of the normal amplitude (*SAR*), that is, these values are obtained by dividing the values in the second column by the values in the first column. Finally, in the last column, N_f indicates the number of verified load cycles until failure (complete separation of the specimen).

It can be seen that the greater the intensity of the amplitudes, the lower the number of verified cycles at the time of fracture. However, there were two cases where at the respective intensity of the normal and shear amplitudes the break did not occur, and the so-called runout was verified. In these cases, the N_f was assigned the value of 1,000,000.

The results presented in Tables 1 and 2 are shown graphically in Figure 3. This plot relates the normal and shear amplitudes as a function of the number of cycles and shows two SN curves per load. This way of plotting the stress amplitudes as a function of the number of cycles is not the conventional one. In the most common representation, the two amplitudes are converted into an equivalent parameter and then correlated with the number of load cycles N_f, resulting in a typical SN curve.

The problem with this approach is that converting the load amplitudes (normal and shear) to equivalent stress requires a scaling factor between the normal and shear stresses (for example, for the von Mises equivalent stress, the scaling factor is the square root of three). This scaling factor can bias the results toward non-proportionality when evaluating the sensitivity factor. It is known that the scaling factor between normal and shear stresses is not independent of the type of stress, the respective intensity, and the number of cycles. Due to this fact, the typical SN curve in the Y parameter approach is decomposed into two components, one for the normal stress and the other for the shear stress. This approach eliminates the limitations described above.

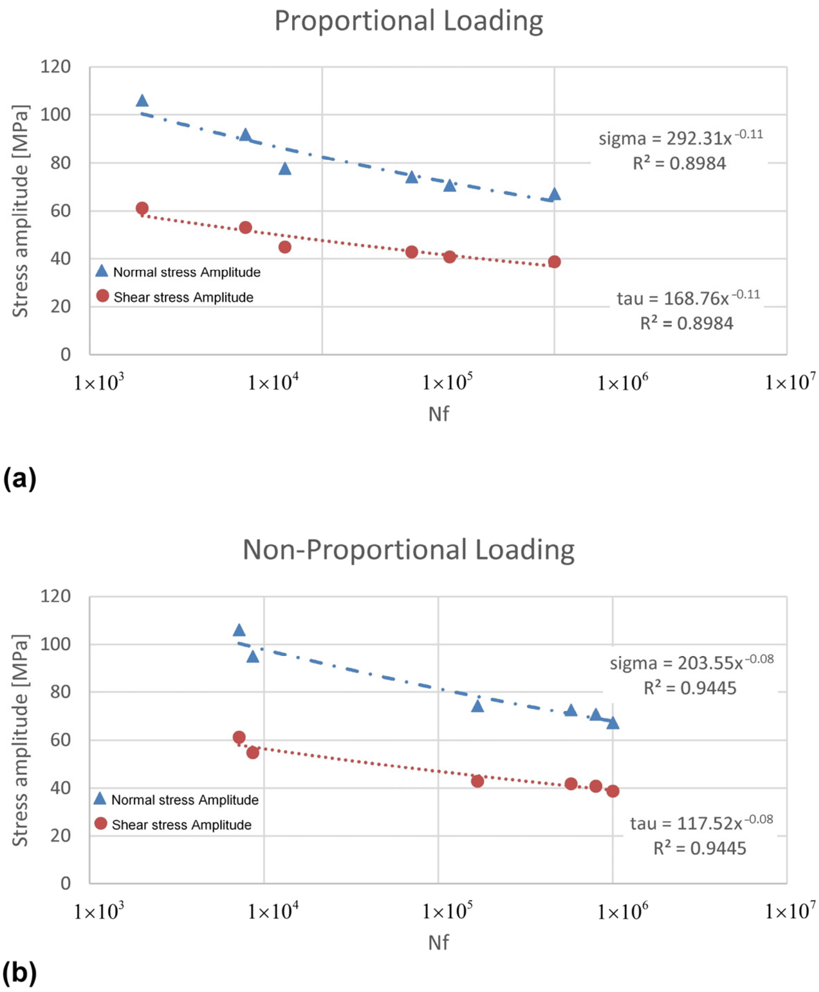

Figure 3. (**a**) Proportional loading results and respective SN trend lines, (**b**) non-proportional fatigue strength and respective SN trend lines.

With the SN curves plotted for both loads, it was possible to determine the expressions for each curve by fitting the experimental results using power equations. Since the plots are of the semi-logarithmic type, the power curves resemble a straight line. Equations (6) through (9) were determined for an R in the interval of 0.89 to 0.94, which is a fairly acceptable deviation from the experimental results. Based on the Equations (6) to (9) and using Expressions (4) to (5) for the calculation of the parameter Y, Equations (10) and (11) are obtained.

$$\sigma_{a,PP} = 292.31 \cdot x^{-0.11}, \tag{6}$$

$$\tau_{a,PP} = 168.76 \cdot x^{-0.11}, \tag{7}$$

$$\sigma_{a,OP} = 203.55 \cdot x^{-0.08} \tag{8}$$

$$\tau_{a,OP} = 117.52 \cdot x^{-0.08}, \tag{9}$$

$$Y_{normal} = \frac{\sigma_{PP}}{\sigma_{OP}} = \frac{292.31 \cdot x^{-0.11}}{203.55 \cdot x^{-0.08}} = 1.4360599 \cdot x^{-0.03}, \tag{10}$$

$$Y_{shear} = \frac{\tau_{PP}}{\tau_{OP}} = \frac{168.75 \cdot x^{-0.11}}{117.52 \cdot x^{-0.08}} = 1.4359258 \cdot x^{-0.03}. \tag{11}$$

Figure 4 graphically represents Equations (10) and (11) as a function of the number of cycles N_f. Due to their similarity, their representation is almost superimposed.

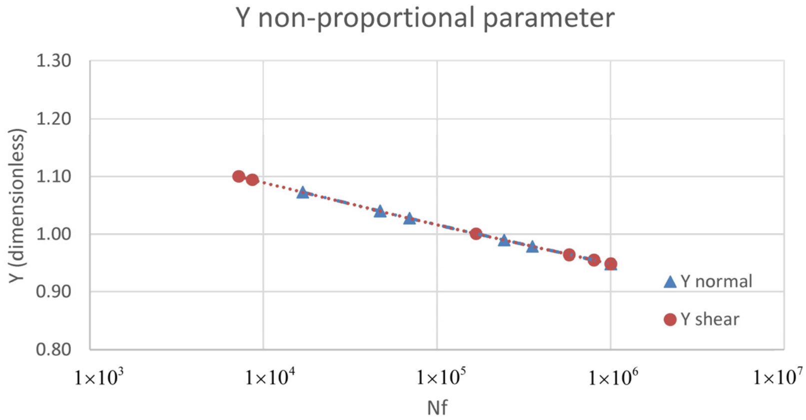

Figure 4. Variation of the Y parameter as a function of the number of loading cycles—magnesium alloy AZ31BF.

Figure 5 shows the plot of parameter Y as a function of the amplitudes of the normal and shear stresses. Based on these diagrams, the expressions for the parameter Y as a function of the amplitudes were determined, see Equations (12) and (13).

$$Y_{normal} = 0.346 \cdot \sigma_a^{0.244}, \tag{12}$$

$$Y_{shear} = 0.2559 \cdot \tau_a^{0.3581}. \tag{13}$$

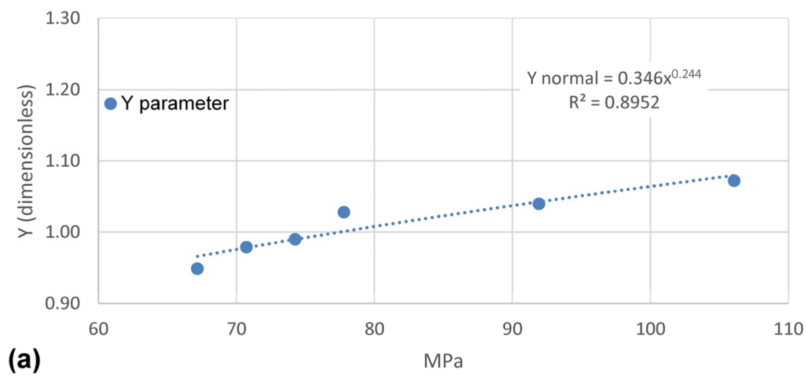

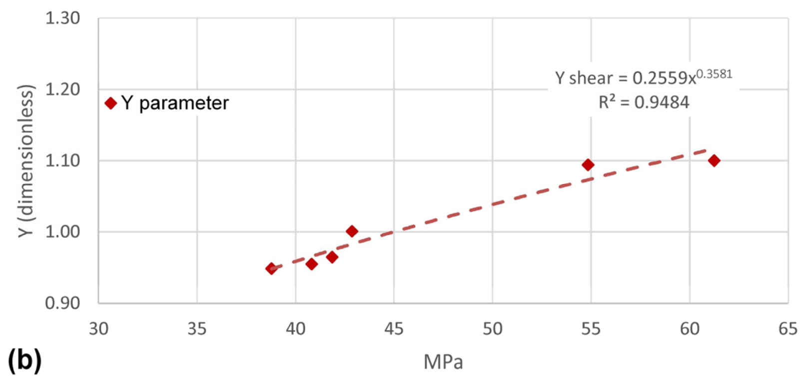

Figure 5. Variation of the Y parameter, magnesium alloy AZ31BF, (**a**) as a function of normal stress amplitude, (**b**) as a function of shear stress amplitudes.

5. Discussion

Based on the results obtained, we can conclude that the damage caused by proportional loads is indeed different from the damage caused by non-proportional loads. The only difference between the two loads considered in this study is the phase shift between the two load channels (normal and shear), i.e., the SAR was kept the same for both loads, leading to the difference in damage due to the phase shift observed in the experimental results. In this sense, damage parameters based only on the intensities of the amplitudes of normal and shear stresses cannot distinguish between proportional and non-proportional damage. The Y parameter proves to be suitable to distinguish the damage caused by both types of loading.

The analysis of Expressions (10) and (11) shows that the difference between the normal Y parameter and the shear Y parameter is indeed negligible for the magnesium alloy AZ31BF. However, it is shown that there are experimental results for other materials where this difference is more pronounced [38]. Based on the plot of these expressions (Figure 4), where the evolution of the non-proportional sensitivity parameter Y is represented, it can be seen that the Y parameter does not remain constant over the number of cycles. Considering that a lower number of loading cycles leads to higher stress amplitudes and a higher number of cycles leads to lower stress amplitudes, it can also be concluded that the parameter Y varies as a function of the intensity of the stress amplitudes (normal and shear).

From Expressions (12) and (13) and the respective plots (Figure 5), it can be seen that the Y value is greater than 1 at higher amplitudes and less than 1 at lower amplitudes. Higher amplitudes lead to higher degrees of deformation and, consequently, to a stronger expression of cyclic plasticity, which proves a greater sensitivity of the AZ31BF magnesium alloy to non-proportionality in this range of stress amplitudes. In this case, the non-proportional load causes more damage compared to the non-proportional load because the non-proportional load amplitudes are smaller and result in the same number of fatigue cycles at the time of failure.

If we analyze the evolution of the parameter Y with the increase of the intensity of the loading amplitude (normal or shear loading, Figure 5), we can identify a loading intensity where the parameter Y equals 1. In this case, the normal amplitude is equal to 77.4 MPa and the shear amplitude is equal to 45 MPa, resulting in a fatigue life of 200,000 cycles. In this particular case, the non-proportional damage is equal to the proportional damage, with no difference in damage between the two loads. Continuing the analysis, we can see that after 200,000 cycles the relationship between the non-proportional and proportional damage reverses, resulting in a Y parameter of less than 1.

In this case, the proportional loading results in greater damage to the AZ21BF magnesium alloy compared to the non-proportional loading, i.e., the amplitudes of the proportional loading are less than the amplitudes of the non-proportional loading for the same fatigue duration. This result leads to the conclusion that approaches to characterize the cyclic response to non-proportional loading cannot be of the constant type. It is important that they consider the intensity of the amplitudes to capture the cyclic response of the material.

In this sense, the alpha parameter presented in the literature, Equation (1), does not capture this variation, which is an extremely important drawback when evaluating the cumulative damage of variable amplitude loading spectra, since its applicability is rather limited to fatigue design for infinite life. In turn, the parameter F, Equation (2), through the ratio between the smallest and largest diameters of the ellipse circumscribing the stress trajectory represented in a given stress space, allows for the consideration of the variation in the intensity of the stress amplitude. However, F estimates may be biased in the case of non-proportionality due to the constant ratio between normal and shear stresses in the stress space where the F parameter is evaluated.

For loading regimes with infinite life under multiaxial fatigue, the Y parameter takes the value 0.95, indicating a very low sensitivity to non-proportionality compared to other materials, e.g., the high-strength steels Ck45 and 42CrMo4 have Y values of 0.83 and 0.95, respectively, and the stainless steel AISI 303 has a Y value of 0.81 [38].

From this we can conclude that the AZ31BF magnesium alloy indeed has a lower sensitivity to non-proportional loading at infinite life and in this respect is on the same level as the high-strength steels.

6. Conclusions

The objective of this study was to evaluate the cyclic response of AZ31BF magnesium alloy when subjected to a non-proportional reference load normally used to characterize fatigue damage due to non-proportionality, i.e., a biaxial load with a phase shift of 90 degrees and a ratio between the normal and shear amplitude of 45 degrees.

The sensitivity of this alloy to non-proportional loading was quantified by the non-proportional sensitivity parameter Y, which is obtained from an expression relating the intensity of normal and shear stresses under proportional and non-proportional loading to the fatigue strength of magnesium alloy AZ31BF.

The results show that the non-proportional sensitivity of magnesium alloy AZ31BF varies as a function of fatigue life, in other words, the non-proportional sensitivity of this alloy varies as a function of the intensity of the normal and shear stress amplitudes.

From the experimental results, it is shown that this magnesium alloy is very sensitive to the non-proportionality at higher amplitudes of the normal and shear stresses, i.e., at higher strains and, consequently, at higher deformations, the Y parameter is greater than 1, which means that for the same stress range at proportional and non-proportional loading, the damage caused by the non-proportional loading is greater. This increase in damage results only from the 90 degree phase shift between normal and shear stress.

On the other hand, with the decrease of the intensity of the normal and shear stress amplitudes and, consequently, with the increase of the fatigue life, a decrease of the parameter Y to values below 1 is observed. The kink point of the damage regime occurs at 200,000 cycles, from which the parameter Y assumes values below 1. In this case, the non-proportional load starts to cause less damage than the proportional load.

From these results, we can conclude that the sensitivity of magnesium alloy AZ31 BF to non-proportional loading is not constant, i.e., it varies depending on the intensity of the amplitudes of normal and shear stresses in a given loading spectrum.

We may also note that constant parameters for non-proportionality, i.e., a non- proportional parameter independent of fatigue strength or, alternatively, a parameter independent of the intensity of the amplitude of the normal and shear stresses, prove insufficient to evaluate the cumulative damage caused by non-proportional loading because the sensitivity to non-proportional loading varies as a function of the intensity of the loading amplitudes. From a practical point of view, the evaluation of the cyclic response of magnesium alloys to non-proportional loading obtained in this study enables the fatigue design of the AZ31BF magnesium alloy components subjected to multiaxial cyclic loading, both from the point of view of infinite life and from the point of view of evaluating cumulative damage in situations with variable loading amplitude spectra.

The limitations of the present study arise from the fact that only the non-proportional reference case was investigated. However, there are other non-proportional loads, namely loads with a phase shift of 30, 45, and 60 degrees, which exhibit an intermediate degree of non-proportionality compared to the reference case. In view of the above and taking into account the peculiarities of the hexagonal compact crystal structure of magnesium alloy AZ31BF, it is hypothesized that the parameter for sensitivity to non-proportionality is a function with two variables, namely the number of load cycles and the phase shift. Investigation of this hypothesis has been deferred for future work.

Author Contributions: Conceptualization, V.A. and L.R.; methodology, V.A.; software, V.A. and F.B.; validation, L.R. and M.F.; formal analysis, L.R.; investigation, V.A.; resources, L.R.; data curation, V.A. and F.B.; writing—original draft preparation, V.A.; writing—review and editing, L.R. and F.B.; visualization, V.A. and F.B.; supervision, L.R.; project administration, L.R.; funding acquisition, M.F. All authors have read and agreed to the published version of the manuscript.

Funding: This work was supported by FCT, through IDMEC, under LAETA, project UIDB/50022/2020.

Conflicts of Interest: The authors declare no conflict of interest.

References

1. Kawajiri, K.; Kobayashi, M.; Sakamoto, K. Lightweight Materials Equal Lightweight Greenhouse Gas Emissions?: A Historical Analysis of Greenhouse Gases of Vehicle Material Substitution. *J. Clean. Prod.* **2020**, *253*, 119805. [CrossRef]
2. Blanco, D.; Rubio, E.M.; Lorente-Pedreille, R.M.; Sáenz-Nuño, M.A. Sustainable Processes in Aluminium, Magnesium, and Titanium Alloys Applied to the Transport Sector: A Review. *Metals* **2022**, *12*, 9. [CrossRef]
3. Contreras Lopez, J.; Chiachío, J.; Saleh, A.; Chiachío, M.; Kolios, A. A Cross-Sectoral Review of the Current and Potential Maintenance Strategies for Composite Structures. *SN Appl. Sci.* **2022**, *4*, 180. [CrossRef]
4. Romano, F.; Sorrentino, A.; Pellone, L.; Mercurio, U.; Notarnicola, L. New Design Paradigms and Approaches for Aircraft Composite Structures. *Multiscale Multidiscip. Model. Exp. Des.* **2019**, *2*, 75–87. [CrossRef]
5. Kermanidis, A.T. Aircraft Aluminum Alloys: Applications and Future Trends. In *Revolutionizing Aircraft Materials and Processes*; Springer: Berlin/Heidelberg, Germany, 2020; pp. 21–55.
6. Prasad, S.S.; Prasad, S.B.; Verma, K.; Mishra, R.K.; Kumar, V.; Singh, S. The Role and Significance of Magnesium in Modern Day Research-A Review. *J. Magnes. Alloys* **2022**, *10*, 1–61. [CrossRef]
7. Song, J.; Chen, J.; Xiong, X.; Peng, X.; Chen, D.; Pan, F. Research Advances of Magnesium and Magnesium Alloys Worldwide in 2021. *J. Magnes. Alloys* **2022**, *10*, 863–898. [CrossRef]
8. Yang, Y.; Xiong, X.; Chen, J.; Peng, X.; Chen, D.; Pan, F. Research Advances in Magnesium and Magnesium Alloys Worldwide in 2020. *J. Magnes. Alloys* **2021**, *9*, 705–747. [CrossRef]
9. Chakraborty Banerjee, P.; Al-Saadi, S.; Choudhary, L.; Harandi, S.E.; Singh, R. Magnesium Implants: Prospects and Challenges. *Materials* **2019**, *12*, 136. [CrossRef]
10. Tecco, S.; Grusovin, M.G.; Sciara, S.; Bova, F.; Pantaleo, G.; Capparé, P. The Association between Three Attitude-Related Indexes of Oral Hygiene and Secondary Implant Failures: A Retrospective Longitudinal Study. *Int. J. Dent. Hyg.* **2018**, *16*, 372–379. [CrossRef]
11. Cappare, P.; Ferrini, F.; Mariani, G.; Nagni, M.; Cattoni, F. Implant Rehabilitation of Edentulous Jaws with Predominantly Monolithic Zirconia Compared to Metal-Acrylic Prostheses: A 2-Year Retrospective Clinical Study. *J. Biol. Regul. Homeost. Agents* **2021**, *35*, 99–112.
12. Gherlone, E.F.; Capparé, P.; Pasciuta, R.; Grusovin, M.G.; Mancini, N.; Burioni, R. Evaluation of Resistance against Bacterial Microleakage of a New Conical Implant-Abutment Connection versus Conventional Connections: An in Vitro Study. *New Microbiol.* **2016**, *39*, 49–56.
13. Anes, V.; Reis, L.; Freitas, M. Evaluation of the AZ31 Cyclic Elastic-Plastic Behaviour under Multiaxial Loading Conditions. *Frat. Ed Integrità Strutt.* **2014**, *8*, 282–292. [CrossRef]
14. Anes, V.; Reis, L.; de Freitas, M. Evaluation of a Phenomenological Elastic-Plastic Approach for Magnesium Alloys under Multiaxial Loading Conditions. *Fatigue Fract. Eng. Mater. Struct.* **2019**, *42*, 2468–2486. [CrossRef]
15. Milner, J.L.; Abu-Farha, F. Microstructural Evolution and Its Relationship to the Mechanical Properties of Mg AZ31B Friction Stir Back Extruded Tubes. *Magnes. Technol.* **2014**, *2016*, 263–268.
16. Albinmousa, J.; Adinoyi, M.J.; Merah, N. Multiaxial Fatigue of Extruded ZK60 Magnesium Alloy. *Fatigue Fract. Eng. Mater. Struct.* **2019**, *42*, 2276–2289. [CrossRef]
17. Gryguć, A.; Karparvarfard, S.M.H.; Roostaei, A.; Toscano, D.; Shaha, S.; Behravesh, B.; Jahed, H. On the Load Multiaxiality Effect on the Cyclic Behaviour of Magnesium Alloys. In *Magnesium Technology 2020*; Springer: Berlin/Heidelberg, Germany, 2020; pp. 151–159.
18. Reza Kashyzadeh, K.; Amiri, N.; Maleki, E.; Unal, O. A Critical Review on Improving the Fatigue Life and Corrosion Properties of Magnesium Alloys via the Technique of Adding Different Elements. *J. Mar. Sci. Eng.* **2023**, *11*, 527. [CrossRef]
19. Wei, H.; Carrion, P.; Chen, J.; Imanian, A.; Shamsaei, N.; Iyyer, N.; Liu, Y. Multiaxial High-Cycle Fatigue Life Prediction under Random Spectrum Loadings. *Int. J. Fatigue* **2020**, *134*, 105462. [CrossRef]
20. Anes, V.; Reis, L.; Li, B.; De Freitas, M. New Cycle Counting Method for Multiaxial Fatigue. *Int. J. Fatigue* **2014**, *67*, 78–94. [CrossRef]
21. Albinmousa, J.; Adinoyi, M.J.; Merah, N. Multiaxial Low-Cycle-Fatigue of Stainless Steel 410 Alloy under Proportional and Non-Proportional Loading. *Int. J. Press. Vessel. Pip.* **2021**, *192*, 104393. [CrossRef]
22. Yankin, A.; Mugatarov, A.I.; Wildemann, V.E. Influence of Different Loading Paths on the Multiaxial Fatigue Behavior of 2024 Aluminum Alloy under the Same Amplitude Values of the Second Invariant of the Stress Deviator Tensor. *Frat. Integrità Strutt.* **2021**, *15*, 327–335. [CrossRef]

23. Skibicki, D.; Pejkowski, Ł. The Relationship between Additional Non-Proportional Hardening Coefficient and Fatigue Life. *Int. J. Fatigue* **2019**, *123*, 66–78. [CrossRef]
24. Branco, R.; Costa, J.D.; Borrego, L.P.; Berto, F.; Razavi, S.M.J.; Macek, W. Comparison of Different One-Parameter Damage Laws and Local Stress-Strain Approaches in Multiaxial Fatigue Life Assessment of Notched Components. *Int. J. Fatigue* **2021**, *151*, 106405. [CrossRef]
25. Ravi, S.K.; Wei, Z.; Dong, P.; Pei, X. Modeling of Non-Proportional Multiaxial Fatigue under Synchronous and Asynchronous Sinusoidal Loading Conditions. *Int. J. Fatigue* **2022**, *163*, 107000. [CrossRef]
26. Yang, S.; Sun, J. Multiaxial Fatigue Life Assessment of 304 Austenitic Stainless Steel with a Novel Energy-Based Criterion. *Int. J. Fatigue* **2022**, *159*, 106728. [CrossRef]
27. Deng, Q.-Y.; Zhu, S.-P.; Niu, X.; Lesiuk, G.; Macek, W.; Wang, Q. Load Path Sensitivity and Multiaxial Fatigue Life Prediction of Metals under Non-Proportional Loadings. *Int. J. Fatigue* **2023**, *166*, 107281. [CrossRef]
28. Gan, L.; Wu, H.; Zhong, Z. Multiaxial Fatigue Life Prediction Based on a Simplified Energy-Based Model. *Int. J. Fatigue* **2021**, *144*, 106036. [CrossRef]
29. Zhong, Z.; Lu, Y. Review: Energy Methods for Multiaxial Fatigue Life Prediction. *J. Harbin Inst. Technol.* **2020**, *27*, 1–9.
30. Socie, D.; Marquis, G. *Multiaxial Fatigue*; SAE International: Warrendale, PA, USA, 1999.
31. Anes, V.; Reis, L.; Li, B.; De Freitas, M. New Approach to Evaluate Non-Proportionality in Multiaxial Loading Conditions. *Fatigue Fract. Eng. Mater. Struct.* **2014**, *37*, 1338–1354. [CrossRef]
32. Albinmousa, J.; Jahed, H. Multiaxial Effects on LCF Behaviour and Fatigue Failure of AZ31B Magnesium Extrusion. *Int. J. Fatigue* **2014**, *67*, 103–116. [CrossRef]
33. Albinmousa, J.; Jahed, H.; Lambert, S. Cyclic Axial and Cyclic Torsional Behaviour of Extruded AZ31B Magnesium Alloy. *Int. J. Fatigue* **2011**, *33*, 1403–1416. [CrossRef]
34. Albinmousa, J.; Jahed, H.; Lambert, S. Cyclic Behaviour of Wrought Magnesium Alloy under Multiaxial Load. *Int. J. Fatigue* **2011**, *33*, 1127–1139. [CrossRef]
35. Zhu, Y.; Hou, D.; Chen, K.; Wang, Z. Loading Direction Dependence of Asymmetric Response of < C+ A> Pyramidal Slip in Rolled AZ31 Magnesium Alloy. *J. Magnes. Alloys* **2022**. [CrossRef]
36. Anes, V.; Lage, Y.E.; Vieira, M.; Maia, N.M.M.; Freitas, M.; Reis, L. Torsional and Axial Damping Properties of the AZ31B-F Magnesium Alloy. *Mech. Syst. Signal Process.* **2016**, *79*, 112–122. [CrossRef]
37. Anes, V.; Reis, L.; Freitas, M. Fatigue Damage Map of AZ31B-F Magnesium Alloys under Multiaxial Loading Conditions. *Metals* **2021**, *11*, 1616. [CrossRef]
38. Anes, V.; Reis, L.; Freitas, M. Effect of Shear/Axial Stress Ratio on Multiaxial Non-Proportional Loading Fatigue Damage on AISI 303 Steel. *Metals* **2022**, *12*, 89. [CrossRef]